INTRODUCTION

Project outline

The focus of this project is on the combination of three-dimensional (3D) models of the liver with soft tissue properties and their use for surgical simulators.

In this introductory section of this project we describe the need for and current uses simulation has in medicine and surgery, as well its advantages over traditional teaching methods, such as cadaveric and animal dissection. From this, we discuss the different types of simulators under development and those which are currently available, focusing particularly on computer-based or Virtual Reality (VR) simulators and the use of haptics of force feedback to improve on the realism of the simulator.

Aims

To create three-dimensional (3D) models of the liver constructed from CT and MR images and to incorporate the relevant tissue properties into these 3D models for the use in VR surgical simulators.

In order to do this it is important to:

➢ Establish a clear and reproducible segmentation criteria based on the anatomy of the liver and surrounding structures

➢ Manually segment CT and MR images of the liver using the segmentation criteria to create detailed 3D geometric models of the liver

➢ Assess the reliability of the segmentation criteria by comparing consecutive attempts from the same data

➢ Assess the accuracy and advantages / disadvantages of semi-automatic segmentation methods by comparing the results of using such methods with those of manual segmentation

➢ Assess the relevant tissue properties from a soft tissue properties database into these 3D models using a simulation framework.

This project comprises the initial stages in the development of a new surgical training system, which will eventually be used to simulate key steps in hepatic surgery.

Hypothesis

The use of in-vivo soft tissue properties in combination with suitable soft tissue models and interface devices can result in a more realistic simulation of soft tissue behaviour for surgical simulation.

Simulation and its Use in Medicine and Surgery

With the introduction of new technologies for diagnosis and management, the increase in media coverage of incidents where lack of surgical expertise has endangered lives and the decrease in availability of cadavers for traditional surgical training, there has been an increased dependency of medical education on simulation technology in the last four decades. Simulation technology can provide a standardised assessment and training system for surgeons at all levels, from medical students to credentialed surgeons, whose surgical skills need retesting at regular intervals throughout their careers.

The growing interest and need for simulation has resulted in these technologies already becoming an integral part of medical education and personnel evaluation, applicable across almost all health care domains. Simulations provide a means of improving health care delivery by assessing professional competence and ensuring that a certain degree of proficiency and confidence is achieved on simulators before operating on real patients. This has the potential for reducing the number of unnecessary complications and medical errors, which occur due to technical failure, and therefore improve patient safety. It is estimated that medical errors may cause 100 000 patient deaths each year in the United States alone (Kohn, 2000).

Issenberg (2005) defined simulation as "a person, device or set of conditions which attempts to present evaluation problems authentically. The student or trainee is required to respond to the problems as he or she would under natural circumstances." In the case of the health profession, a simulator usually refers to "a device that presents a simulated patient (or part of a patient) and interacts appropriately with the actions taken by the simulation participant." (Gaba, 2004).

Simulations mimic events that arise in professional encounters, in which professionals are "immersed" in a task and can see the consequences similar to those seen in real situations. This in turn requires the user to respond in an interactive manner as they would do in the real environment. Simulation provides a controlled environment which frees teachers and pupils from the added pressures of operating on real patients during teaching. A simulator must be realistic (Dawson, S L. 1998), which can be achieved when the image has high resolution, the object is deformable when grasped and the surgeon's hand and instruments must interact realistically with the virtual organs. The organs must also have appropriate reactions when manipulated or cut, such as bleeding (Satava, 1993). Learners can manipulate, clip and cut virtual tissues in a virtual environment, which resembles the operating room, with the opportunities to make and correct mistakes as well as attempt tasks multiple times, without jeopardizing patients or causing them unnecessary discomfort.

This is in comparison to traditional surgical training methods, which involve the use of cadavers, live or dead animal tissues and/or inanimate models, all of which vary in their anatomy and physiology (Liu, 2001), allow for only one attempt of a task at a particular anatomical site and do not allow a learner to correct their mistakes. There is

also the added issue of animal rights, which makes the use of animals for training purposes difficult. With the opportunities to practice on "real" patients diminishing, simulators are providing a means for surgical training to deviate away from the old apprenticeship model of "see one, do one, teach one' introduced by Sir William Halsted (Haluck, 2000), thus allowing individuals to practice repeatedly until a certain level of proficiency is achieved prior to participating in live cases. This has become particularly important over the past few decades with incredible advances in minimally invasive surgery, such as laparoscopic cholecystectomy, the skills for which can not be accommodated by the apprenticeship model.

Simulators offer a means of assessing surgeons' performance in an unbiased objective manner, with assessment parameters including time taken to complete a task, number of errors made and path length for each hand (Aggarwal, 2006b). Studies have demonstrated that surgeons, who have undertaken simulation training, have had a significant reduction in their errors and faster performance, than those who did not receive simulator training (Grantcharov, 2004). Studies have demonstrated that repeated practice on simulators improves operating room performance (Seymour, 2002) (Grantcharov, 2004) and simulators can provide novices with levels of skills similar to experienced laparoscopic surgeons (Aggarwal, 2006a).

The first prototypes of virtual reality surgical simulators have been around since the laparoscopic era of the 1990s (Delp, 1990). As computer graphics and visualisation have rapidly advanced over the past three decades, so has the development of simulators across multiple fields of medicine. Simulation has proved its use in training professionals in highly hazardous and complex professions, such as virtual cockpit flight simulators to train astronauts and pilots as well as teaching non-hazardous skills, such as teaching medical students how to provide smoking cessation counselling using simulated patient instructors (Eyler et al, 1997).

Simulation has contributed considerably to aviation training in the last four decades, beginning with the Link Flight Simulator. Due to the increased degree of realism of aircraft-specific simulators, pilots spend a significant part of their training programme in simulators. In 1997, Boeing's first 777 aircraft was flown perfectly by a pilot who had spent 1000 hours in an aircraft-specific simulator before ever setting foot in an aircraft.

One of the earliest examples of medical simulations was 3D visualisation of CT images (Herman, 1977). Since then, there has been the introduction of simulators in various fields, such as laparoscopy, endoscopy and hepatic surgery (Marescaux, 1998). Current surgical simulators owe their existence to these pioneering developments in the 1990s and advances in this field continue to be made.

There are several types of patient simulators:

1) A mannequin based simulator ~ this uses a patient mannequin in actual physical reality.

2) A screen based simulator ~ this is on a computer screen only

3) A virtual reality (VR) simulator ~ this uses virtual reality by which parts of or all of the patient and environment are presented to the user through two or three dimensional visual and audio representations, with or without haptics to create a more "immersive" experience. VR simulators may replicate particular procedures, such as laparoscopic surgery (Gaba, 2004).

We will focus on VR simulators for the remainder of this project and in particular the role haptic technology plays in VR simulation.

Virtual Reality Simulators

Virtual reality refers to a "computer-generated representation of an environment that allows sensory interaction, thus giving the impression of actually being present" (Coleman, 1994). This is achieved by "immersing" the learner's senses into the "virtual world" (Satava, 1993). A VR reality simulator consists of a mono- or stereoscopic display (either a cathode ray tube or head-mounted display), a PC or more powerful computer, and an interface device, which allows the user to interact with the simulation environment in a realistic manner (Sorid, 2000).

Commercial simulators are available for practicing tasks such as laparoscopic cholecystectomies as well as threading flexible endoscopes down a virtual patient's throat**.**

Fig 1: MIST-VR® (Aggarwal, 2004).

VR simulations can be divided into three categories (figure 5):

➢ **First Generation Simulators**
These describe the geometry of anatomy alone and the trainee can navigate within a "virtual patient", but with a limited number of interactions.

➢ **Second Generation Simulators**
These include first generation simulator characteristics, as well as the modelling of physical properties of living tissues. These simulators incorporate haptic feedback, where biomechanical properties are incorporated to allow realistic
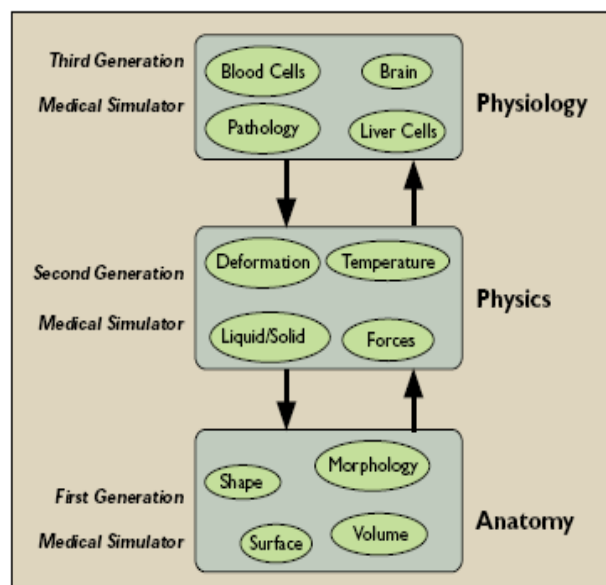

Figure 5: Different generations of simulators (Delingette, 2005)

interactions between surgical instruments and tissues.

➢ **Third Generation Simulators**
These combine anatomical, physical and physiological properties, such as bleeding. This means functions of various organ systems can be incorporated into these simulators. Haptic and visual feedback can also be incorporated into these simulators (Delingette, 2005).

We now briefly discuss some of the currently available commercial VR simulators.
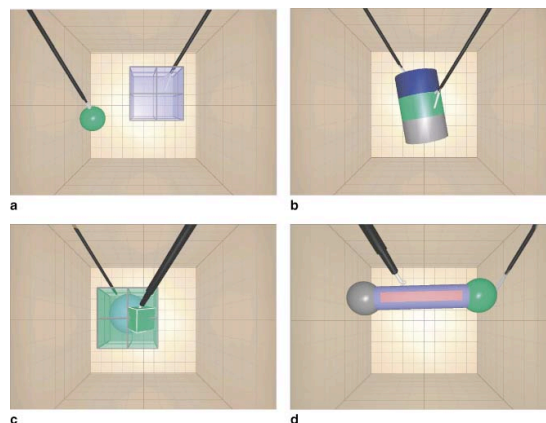
MIST-VR® (Mentice)

Fig 2: MIST-VR® (Aggarwal, 2004).

The Minimally Invasive Surgical Trainer- Virtual Reality or MIST-VR, is a well established laparoscopic simulator designed by Mentice, a Swedish company. MIST-VR® comprises two standard laparoscopic instruments held on a frame with position-sensing gimbals (Wilson, 1997), which are linked to a Pentium® personal computer Movements of these instruments are relayed in real time to a computer monitor. MIST-VR® has abstract tasks, which involve the random appearance of targets on the screen, which can be manipulated and 'grasped'. MIST-VR® teaches the basic skills needed for all types of minimally invasive surgery and a learner's time, error rate and economy of movement for each and can be measured. (Aggarwal, 2004). MIST-VR® is a product for training and assessing surgical laparoscopic psychomotor skill (Figure 1) (Figure2).

LapSim® (Surgical Science)
This laparoscopic trainer has more realistic tasks than MIST-VR®, involving physiological processes, such as bleeding into deformable structures. Lapsim® simulates the steps involved in grasping, cutting and clipping of structures. Execution time, extent of tissue damage and instrument path length can be recorded for a surgeon (Carter, 2005) (Figure 3).

Fig 3: LapSim® (Aggarwal, 2004).

LapMentor™ (Simbionix)
This simulator provides a tutorial on how to perform a laparoscopic cholecystectomy, which they can then perform with the benefit of haptic feedback on simulated patients with various pathologies.

GI Mentor™ (Simbionix)
This simulator can simulate gastrointestinal endoscopies and endoscopic ultrasounds, providing trainees with basic psychomotor endoscopy skills and enabling them to practice endoscopic procedures on a mannequin with a mouth and rectum. The simulation computer provides force feedback. The trainee can practice on simulated patients with various pathologies and anatomy and various skills, such as completion task can be assessed (Figure 4).

Fig 4. GI Mentor II. (Koch, 2008)

Haptic Technology

With the increased need to incorporate haptic feedback into simulators in order to improve their realism, we shall turn our focus to haptic feedback.

In the past decade, the need for and interest in haptic technology has increased enormously. Haptics is derived from the Greek, haptesthai, meaning to touch, and in the early 20th Century, the word haptics was introduced to broadly refer to touch interactions that occur for the purpose of perception and manipulation of objects (Salisbury, 2004). Gregory Burdea introduced a portable force-feedback glove in the early 1990s. Since then technology has evolved to allow more complex haptic interactions to be established.

It is thought that the primary source of information that a surgeon relies on during a procedure is the sense of touch (Plinkert, 1998). Touch permits the surgeon to apply appropriate tension during dissection, while avoiding tissue damage. Haptics can create a more realistic environment, the skills from which can be translated by a surgeon into the operating room (Bholat. 1999).

Computer haptics enables the interaction of humans with simulated objects displayed in a manner which allows these objects to be physically palpated. The interaction between a human hand and a simulated object is facilitated by haptic interface devices, which allow users to touch 2D and 3D objects in virtual environments.

The haptic interface allows new sensory display modalities to present information to the human, by exerting controlled forces on the human hand. Haptic interactions are bidirectional, with information and energy flowing to and from the operator.
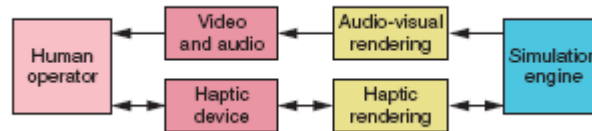

Figure 6: Basic architecture for virtual reality application incorporating visual, auditory, and haptic feedback. (Salisbury, 2004)

A virtual reality simulator must consist of several components in order to elicit auditory, visual and haptic feedback (Figure 6). The simulation engine is responsible for computing the virtual environment's behaviour over time, whilst the sound, force and graphics of the virtual environment are directed towards the operator via auditory, visual and haptic rendering algorithms. Transducers then convert the auditory, visual and force signals from the computer into a format, which can be perceived by the operator (Salisbury, 2004).

Haptics can be divided into two main categories of sensory information: tactile information, which refers to pressure information acquired through mechanoreceptors in the skin. Tactile information provides us with information about surface texture and shape. The second main category is kinaesthetic information, which refers to information about physical forces acquired through joint sensors, which creates the feeling of motion in the body. It is a combination of these two which allows for the perception of interaction forces.

There are a number of haptic devices currently available:
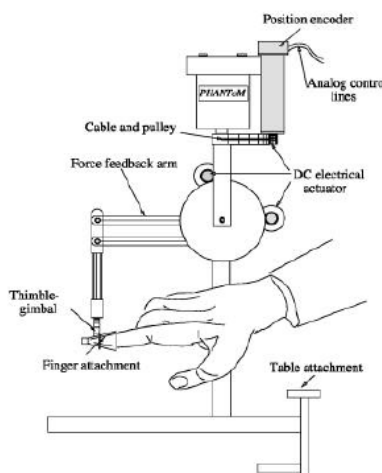
PHANTOM® (SensAble)

The PHANTOM was first introduced in the 1990s and this series of haptic devices are currently the most popular haptic feedback interfaces. This device resembles a robotic arm with a surgical instrument attached. This device relays the position of this arm to a PC. The software, GHOST, translates elasticity and roughness into commands for the arm, and a force needed to simulate the virtual environment is produced (Figure 7-8). The PHANTOM is the haptic device used inside this project's simulator.

Figure: 7
The PHANTOM Arm (adapted from Massie and Salisbury, 1994. ASME)

Figure 8: The PHANTOM Omni.
(http://www.sensable.com/haptic-phantom-omni.htm accessed 16/04/08)

Haptic Workstation (Immersion)

This 3D haptics innovation is a fully integrated simulation system, which provides right and left-hand force feedback and enables the user to experience an immersive experience via tits head-mounted display.

Figure 10: The Haptic Workstation

(http://www.immersion.com/images/right/haptic_workstation.jpg accessed 16/04/2008)

Immersive Workbench (SenseGraphics)

The Immersive Workbench is a haptic device which functions using a high resolution 3D stereo projector. It enables movement tracking and allows trainees to visualise and touch objects in a virtual work volume.

Figure.
www. SenseGraphics.com

LapMentor and GI Mentor, as mentioned earlier, are just two examples of simulators, which use haptic feedback. Another simulator which uses haptic feedback is ProMIS™ (Haptica), which enables users to interact with virtual and physical models, therefore providing them with skills and techniques necessary for minimally invasive surgery (Figure 11).

Figure 11: ProMIS http://www.haptica.com/id44.htm

Biomechanical Properties of tissue

Most of today's medical simulators do not take into account the physical nature of soft tissues, which make up the majority of the human body. Every soft tissue has an assigned mass, elasticity and viscosity and these parameters determine the appearance of any deformation. It is important to represent the physical properties of tissues in order to produce realistic soft tissue models and enhance the credibility of simulators. Computerised Tomography (CT) and Magnetic Resonance Imaging (MRI) provide accurate anatomical representations of organs and can be used to construct 3D visualisations using computer graphics. Computer graphics enable the incorporation of elastodynamic behaviour into VR models of organs, which enhances the illusion of realism by allowing the surgeon to manipulate tissues using surgical instruments. The development of these 3D models of soft tissues relies on the use of specific

mathematical models and the knowledge of the tissue's mechanical properties, such as tension and rigidity. Soft tissues have deformable behaviour, that is to say their shape can be altered by pressure or stress. It is necessary to model the deformability of soft tissues under the influence of neighbouring structures and surgical instruments (Delingette, 1998). In 1986, Terzopoulos developed the first deformable model by incorporating physical properties directly into a graphical object (Terzopoulos, 1987).

There are a number of existing models which simulate the dynamics of deformable organs, two of which are the spring-mass model, which gives an approximation of the real soft tissue physical behaviour and the second model is the Finite Element Method (FEM), which is the most accurate method for modelling elastic deformations of non-rigid soft tissues due to external influences.

Spring-Mass Models

Spring-Mass Models are the most widely used deformable models applied to surgery simulation. They are a special and simplified version of FEM, however, despite being faster than FEM modelling, spring-mass models are less realistic. These models are based on meshes composed of springs and mass points (Meier, 2005) (Figure 12). The whole mass of the virtual organs for example, is divided up between the mass points of the model, which are represented by nodes in a mesh.
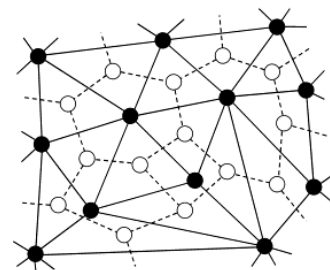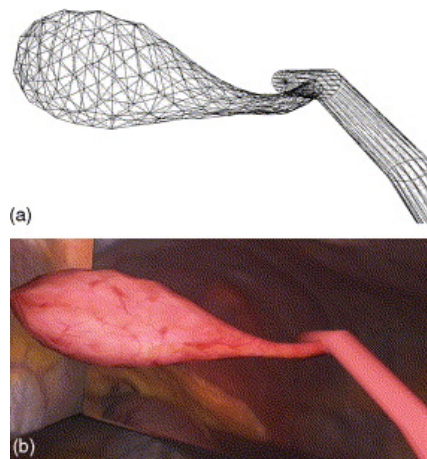
Figure 12: A spring-mass type mesh (Meier, 2005)

These nodes are connected to their neighbours elastically and/ or viscously and these connections are represented by springs. Manipulations, such as incisions or suturing are easily represented using these models. Deformations can be performed virtually by applying external forces, from surgical instruments for example, to these nodes. The node displacement and resulting forces can be calculated (Radetzky, 2000) (Figure 13).

Figure 13: Deformation of a gall bladder modelled with a spring-mass model. (Meier, 2005).

Finite Element Models (FEM)

FEM is considered the more accurate model for simulating organ deformations; however the high computational nature of FEM makes such modelling technique impractical in most cases, especially for real-time simulations of complex objects. The virtual organ's space is tessellated into finite pieces, such as tetrahedrons or cubes. A
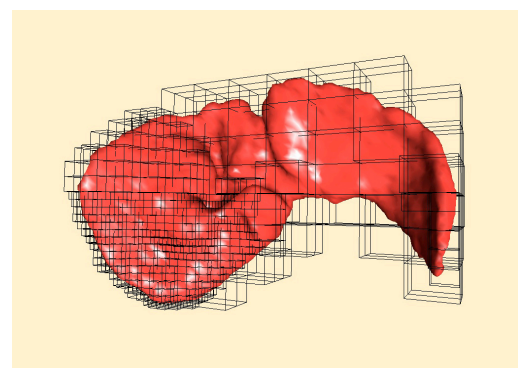
Fig 14. FEM of the liver. (Nesme, 2006).

mathematical model description is then constructed (Radetzky, 2000).

Human organs have non-linear behaviour and therefore a non-linear model of FEM can be used to take into account the varying physical parameters depending on time and space. Non linear FEM can accurately model non-linear elasticity with large deformations in soft tissues (Wu, 2001) (Figure 14).

There are several properties that can be incorporated into simulation models of organs. As mentioned earlier, elasticity is one of them, as is viscosity. Some possible parameters are listed and defined in table 1.

Tissue parameter	Definition
Elasticity	The extent to which an object deforms under stress, but then returns to its original shape when stress is removed.
Viscosity	This is a measure of the resistance of a fluid to being deformed by either stress.
Poisson's Ratio	It is the ratio of the relative contraction strain divided by the relative extension strain.
Young's Modulus	This is a measure of a material's stiffness. It is the ratio of stress over strain in a region, in which Hooke's Law is obeyed for the material.
Hooke's Law	This is an approximation that states that the amount by which a material body is deformed is linearly related to the stress causing the deformation.
Cutting force	Force applied to cut tissue
Friction Force	This is the force between the instrument and tissue
Stress-strain relationship	Stress is the force applied to the tissue. Strain is the change in a structure's dimensions (deformation). ➡ The variation of the elasticity
Ultimate tensile strength	This is the amount of stress that can be applied before a material breaks.
Mass density	The mass of unit volume of a material)kg m^{-3}

Table 1. Some tissue parameters which can be incorporated into simulation models of soft tissues.

**Hooke's Law
(Put this diagram somewhere)**
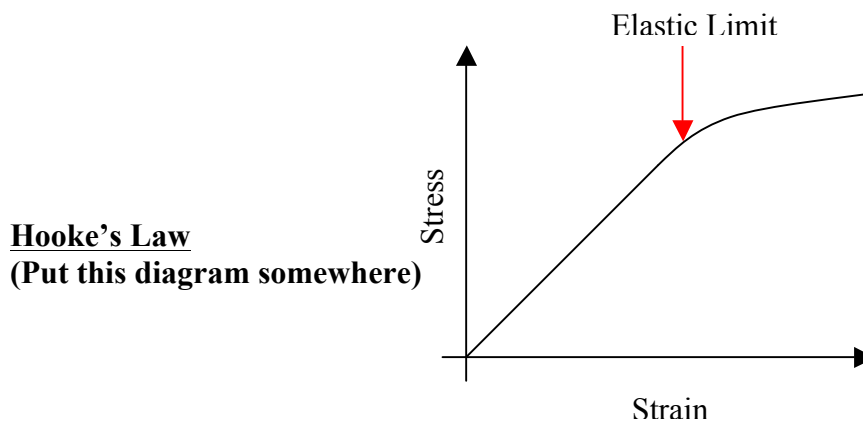
Importance of the liver

The liver is a complex and variable organ. While there has been a vast amount of research regarding visualisation and surgical planning for liver procedures, real time simulation of liver behaviour for surgical simulation is still very challenging. It is important to develop a hepatic surgical simulator which can be applied to all patients, that enables pre-surgical planning, training and teaching about the liver's anatomy.

Segmenting numerous CT and MR image datasets of patient livers and constructing 3D models of the liver, which incorporate various soft tissue properties, is the first step towards creating a realistic hepatic surgical simulator that could be used for laparoscopic hepatic surgery. A hepatic surgery simulator incorporating soft tissue deformable properties and haptic feedback would provide surgeons with a comprehensive visualisation of the liver, allowing them to appreciate the complex anatomy of the liver and to accurately locate pathology. It would also enable surgeons to understand and visualise the relationship of the liver to the associated vasculature, biliary ducts and surrounding anatomy pre-surgically, thus allowing the surgeon to plan the best surgical approach. The ability to practice hepatic surgical procedures repeatedly before attempting the procedure on a real patient will have a huge impact on surgical training and education. 3D visualisations of the liver would allow surgeons to see and gain precise knowledge about crucial structures and elements of the liver that were formerly unseen (Marescaux, 1998).

METHODS AND MATERIALS

Subjects

In order to construct 3D hepatic models, 7 anonymous patients' CT and MRI scans were obtained from the Royal Liverpool Hospital (RLH) and 1 from the Centre Léon Bérard (CLB) each image taken at a different stage in the patient's breathing cycle.

CT and MRI acquisition protocols (this section is to be completed)

The time taken to scan patients was limited as to ensure patients were comfortable and consequently resulted in as little movement as possible and therefore minimise the presence of motion artefacts. The motions of the cardiopulmonary system and the bowel can also produce image artefacts. Segmentation requires high spatial resolution and contrast in order to distinguish structures which are associated with the liver, from those which are not. It was also important when selecting CT and MR images for them to have a high signal to noise ratio (SNR).

The choice of protocols for the selection of CT and MR images with an adequate quality for segmentation were decided upon discussion with radiologists and MR radiographers at CLB at the RLH.

Segmentation

Segmentation is defined as the process of partitioning a digital image into multiple regions and assigning labels to voxels with an identifier (Vidal, 2006). Segmentation of the liver and associated structures in medical images is a fundamental task in the development of 3D visualisations. Before the segmentation process can be initialised, a thorough understanding of the relevant anatomy, i.e. the liver and associated blood vessels and the imaging techniques is required.

The first steps in the construction of a new surgical training simulation involve the creation of highly detailed models of the liver and associated blood vessels. Patient-specific CT and MR images were interpreted and then the liver and associated blood vessels were segmented using a program called Insight Snap visualisation tool kit (ITK-SnAP) (Paul, 2004). This process was highly dependent on the spatial resolution and contrast of the imaging data.
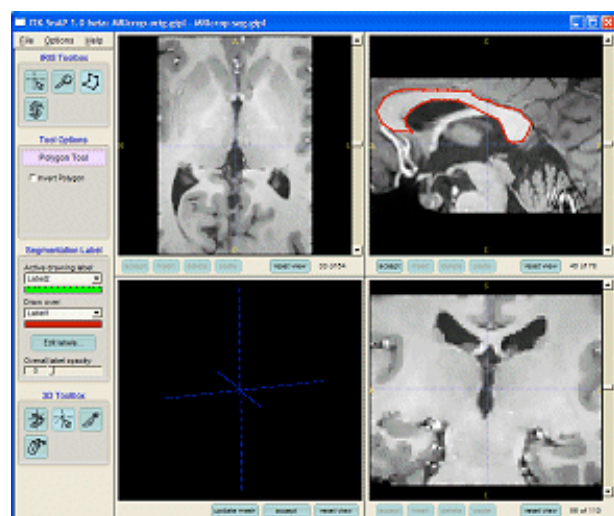

Figure18: ITK-snap: the three orthogonal planes and 3D window
http://www.itksnap.org/docs/viewtutorial.php?chapter=TutorialSectionIntroduction accessed 17/04/08

Segmentation Criteria

Defining the segmentation criteria is one measure that can diminish the discrepancies that occur between successive segmentations of the same data sets.

The liver is a wedge-shaped organ situated in the upper right part of the abdominal cavity. Its base is directed to the right and the thin edge towards the left. The liver possesses three surfaces; the superior, inferior and posterior.

Superior surface

This convex surface is attached to the underside of the diaphragm, which separates the liver from the lower part of the lungs, pleura, heart and pericardium. Centrally this surface consists of a cardiac impression. The superior surface also attaches to the anterior abdominal wall via the falciform ligament. The line of attachment of the falciform ligament divides the liver into the left lobe and bigger right lobe and the superior surface comprises a part of both lobes (Figure 15).
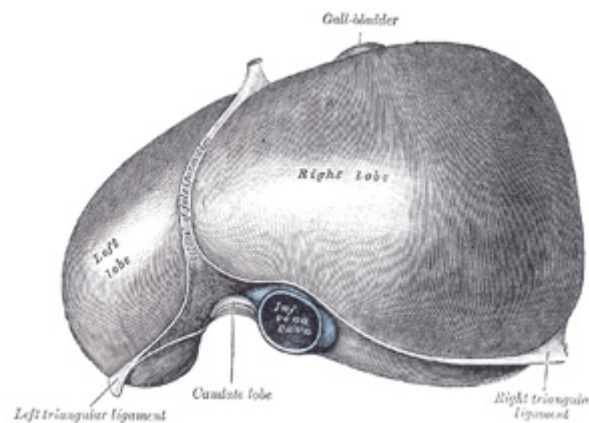

Figure 15: Superior surface of the liver (Gray's Anatomy).

Inferior surface

This surface is concave and directed downwards, backwards and to the left. It is related to the stomach, duodenum, right colic flexure, the right kidney and suprarenal gland. The inferior surface of the left lobe contains the gastric impression from the antero-superior surface of the stomach
The under surface of the right lobe is divided by the fossa for the gall bladder into the smaller quadrate lobe to the left and the caudate lobe to the right (Figure 16).
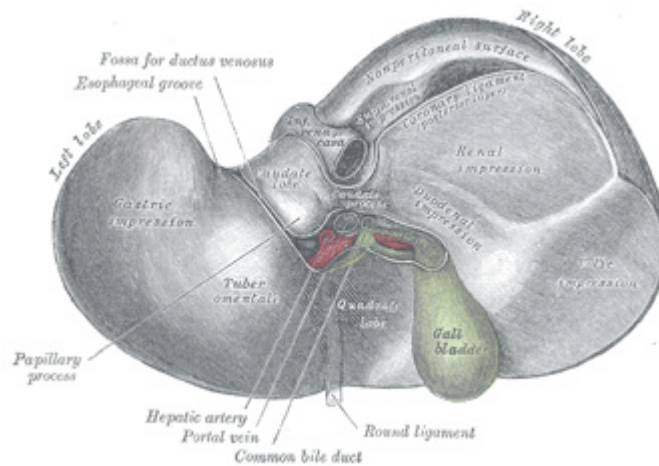
Figure 16: Inferior surface of the liver (Gray's Anatomy).

Posterior surface

This rounded surface is broad behind the right lobe, but narrow on the left. It is marked off from the upper surface by the line of reflection of the upper layer of the coronary ligament, and from the under surface by the line of reflection of the lower layer of the coronary ligament. The central part of this surface is concave and moulded around the crura of the diaphragm and the vertebral column. To the right og this the inferior vena cava in its fossa between portion of the posterior surface which is not covered by peritoneum, and the caudate lobe. The uncovered portion is in direct contact with the diaphragm (Figure 17).
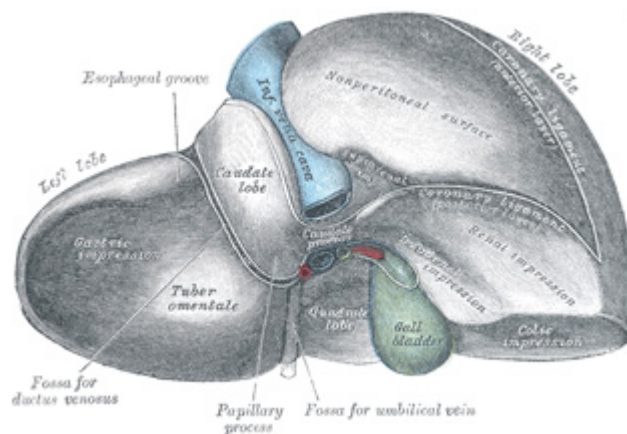

Figure 17: Posterior and inferior surfaces of the liver (Gray's Anatomy)

Right lobe

This is the largest lobe of the liver and occupies the right hypochondrium. It's under and posterior surfaces are marked by fossae for the porta, gall bladder and the inferior vena cava. The left part of this lobe is separated into the quadrate and caudate lobes by the gall bladder fossa.

Quadrate lobe

This lobe is situated on the underside of the right lobe and is bound in front by the anterior margin of the liver; behind by the porta; on the right, by the gall-bladder fossa; and on the left, by the umbilical vein fossa.

Caudate lobe

This is situated on the posterior surface of the liver's right lobe. It is bounded below, by the porta; on the right, by the fossa for the inferior vena cava; and, on the left, by the fossa for the ductus venosus.

Blood vessels

The vessels connected with the liver are the hepatic artery, hepatic veins and the portal vein. The hepatic artery and portal vein ascends to the porta and are in close proximity with the bile ducts and lymphatic vessels, which descend from the porta; the bile duct lies to the right, the hepatic artery to the left and the portal vein lies behind and between these two structures.

Segmentation Tasks

There are three main categories of segmentation; manual, semi-automatic and automatic segmentation.

Task One- Manual Segmentation

ITK-SnAP was installed onto an ordinary desktop PC. ITK-SnAP is an open-source software application for the segmentation of anatomical structures in medical images, such as CT and MR images. The data sets could be visualised in three orthogonal slice planes through the CT and MR images; axial, coronal and sagittal planes (Figure 18). The process of manual segmentation involved revising the anatomy of the liver and related blood vessels in order to differentiate these structures from surrounding unrelated structures and subsequently not include these in the segmentation.
The boundaries of consecutive slices of the liver, hepatic artery, hepatic veins and the portal vein were traced around in the axial window using the manual delineation mode in ITK-SnAP. Segmentation labels were then applied to the liver and associated blood vessels. The segmentations were then adjusted in the coronal and sagittal planes and 3D meshes were constructed from the segmentations, by stacking the sequential slices. The 3D mesh is displayed in the fourth display panel and could be interactively visualised from any viewpoint. The presence of four display windows at once, provides the user with maximum amount of detail about the voxel under the cursor (Figure- results section). The following data sets were segmented: (**Table ?)**

Data set	Image type
CLB_001	CT
RLH_001	CT
RLH_002	CT
RLH_004	CT
RLH_007	CT
RLH_013	CT
RLH_014	MRI
RLH_015	CT

The computing time taken to segment each data set was recorded and the times to segment the initial data sets were compared to the times taken to segment the final data sets **(Graph 1- results section)**.

Task Two- Re-segmentation

Several weeks later, three of the subject's data sets were chosen to be re-segmented by the same operator using ITK-SnAP. These comprised of 2 CT scans (RLH_002, RLH_004) and 1 MRI (RLH_014). The data sets for re-segmentation were chosen for their high quality resolution, good contrast and the liver and the associated blood vessels were easily distinguishable from the surrounding structures.

The computing time taken to re-segment each data set was recorded and the times to re-segment the initial data sets were compared to the times taken to segment the final data sets. The re-segmentation times for these data sets were compared for the times taken to segment them initially **(Graph 2)**.

The re-segmentation process was faster due to familiarity with the ITK-SnAP software, taking on average 3 hours compared to 5-8 hours for the first segmentation attempt.

Task Three- Semi-automatic segmentation

a) Semi-automatic segmentation using ITK-SnAP

ITK-SnAP provides an alternative method of segmenting CT and MR images. This method is known as semi-automatic segmentation, which uses the level set method. This process involves the user placing one or more bubbles in the image and these bubbles grow constrained by intensity edges in the image. This is a numerical technique for tracking interfaces and shapes. This method involves the representation of a surface under the control of a Partial Differential Equation on a volume (Vidal, 2006). Using the ITK-SnAP semi-automatic segmentation method meant we were able to compare the resulting segmentation to the manual segmentation for the same data set.

RLH_004 was segmented using this semi-automatic segmentation method and the computing time taken to semi-automatically segment RLH_004 was recorded and compared to the time taken to manually segment the same data set (**Graph 3)**.

b) Semi-automatic segmentation using Hierarchical Segmentation software

Hierarchical segmentation involves the placement of green seeds inside the liver, thus marking the foreground and then the placement of red markers outside the liver in the background. Hierarchical segmentation depends on the differentiation of 2 adjacent anatomical regions, by comparing the intensity of these regions. The greater the difference in the intensity of these two regions means the edge between the two regions will be stronger and these two regions will be recognised as different anatomical structures (Griffen, 1994). The regions of the image marked with green markers were then stacked upon each other and a 3D mesh was constructed. 20 slices from RLH_004 were re-segmented using hierarchical segmentation software. These consisted of the top 10 slices and the 10 middle slices from the middle of the liver. The top 10 slices of the liver were chosen to be re-segmented as their boundaries were easy to differentiate from the surrounding structures and therefore segmentation was easy. The middle 10 slices were chosen as they were boundaries were difficult to distinguish from the surrounding structures.   The time taken to segment the top 10 slices and the middle 10 slices using hierarchical segmentation was recorded and compared to the time taken to segment the same slices using the ITK-SnAP manual segmentation technique.

   Hierarchical segmentation was then used to segment the top 20 slices of an MRI data set (MRI-014). The time taken to segment this data set was recorded every 5 slices and compared to the time taken to segment the same slices using ITK-SnAP manual-segmentation. This MRI was chosen in order to compare the differences which occur between segmentation of a CT scan and a MRI scan, such as the length of time taken and the ability to distinguish between the relevant structures and their surroundings.

Table 2. Segmentations to be compared.

Segmentation 1	Segmentation 2 (Comparison segmentation)
RLH_002_Manual	RLH_002_Re-segmentation
RLH_004_Manual	RLH_004_Re-segmentation
RLH_014_Manual **(MRI)**	RLH_014_Re-segmenation
RLH_004_Manual_top 10 slices	RLH_004_Hierarchical_top 10 slices
RLH_004_Manual_middle 10 slices	RLH_004_Hierarchical_middle 10 slices
RLH_014_Manual_19 slices	RLH_014_Hierachical_19 slices
RLH_004_Manual	RLH_004_Level set

Task Four- Mesh generation

Marching Cube

Using a high resolution algorithm, known as marching cube, a 3D mesh was generated from the segmentation data **(Lorensen, 1987).** Marching cube involves the division of the liver into numerous cubes. These virtual cubes' vertices are defined by the centres of eight CT scan voxels. For each of them, the information about material is obtained directly from the intensity of the 3D segmented images. If a vertex has different material information from its neighbours, a boundary surface exists between them, which separates different materials. This processing of generating a surface is rapid due to the direct triangulation from the look-up-table properties of the marching cube routine. **(Figure of marching cubes)**

Mesh Alignment

The liver segmentations to be compared (table 2) were then matched up and processed using a general-purpose mesh processing software program, called MeshLab. MeshLab enables alignment of the comparison meshes. MeshLab uses an iterative alignment algorithm, the ICP algorithm, which works in three phases. Firstly, it establishes correspondence between pairs of features in the two structures that are to be aligned based on proximity **(Figure of this)**. Secondly, the rigid transformation that best maps the first member of the pair onto the second using a mean square cost function is estimated. And finally, the resulting transformation is applied to all features in the first structure. These three phases are repeated until convergence is concluded.

Task Five- Analysis using validation tool M.E.S.H.

Using M.E.S.H (Measuring Error between Surfaces using the Haussdorf distance), comparisons were made between the manual re-segmentations and original manual segmentations; the hierarchical segmentations and original manual segmentations; the level-set segmentations and the original manual segmentations. M.E.S.H measures distortion between two discrete surfaces and uses the Haussdorf distance algorithm to compute minimum, maximum, mean and root-mean-square errors between the two segmentations **(Reference:http://mesh.berlios.de/).** Every contour point is compared to all the other ones in the complex 3D image. M.E.S.H presents a colour-coded display to demonstrate the different distances between the contours in the different segmentation attempts. The blue parts of the resulting 3D image represent the smallest distances between the contours in the original segmentation and the comparison segmentation; whilst red represents the largest difference between the two segmentations being compared **(Figures 1-7 results)** **(Graphs 5-6 results section)**.

RESULTS

Task One and Two- Manual Segmentation and Re-segmentation.

(Image – demonstration of the steps involved)

Step 1- Tracing around the boundaries of consecutive slices of liver.
Step 2- Application of segmentation labels.
Step 3- Stacking of sequential slices.
Step 4- Construction of 3D mesh.

After tracing around the boundaries of consecutive liver slices and applying segmentation labels, the following 3D model was constructed for data set 004 using ITK-SnAP manual segmentation (Step 4- inferior/ superior / different views of the same liver reconstruction; match up to the grey's anatomy pictures).

The models obtained were 3D reconstructions of the liver consisting of the external surface morphology

The results of the segmentation computing times indicate that the length of time taken to segment

Patient Number	Manual Computing Time (minutes)	Manual Computing Time Reseg (minutes)	Level Set Computing Time (minutes)
CLB_1 (Resp. breath 1)	243	-	-
CLB_1 (Resp. breath 2)	216	-	-
CLB_1 (Resp. breath 3)	183	-	-
CLB_1 (Resp. breath 4)	147	-	-
CLB_1 (Resp. breath 5)	139	-	-
CLB_1 (Resp. breath 6)	136	-	-
CLB_1 (Resp. breath 7)	131	-	-
CLB_1 (Resp. breath 8)	127	-	-
CLB_1 (Resp. breath 9)	120	-	-
CLB_1 (Resp. breath 10)	117	-	-
RLH_001	252	-	-
RLH_002	236	185	-
RLH_004	227	170	12
RLH_007	212	-	-
RLH_013	205	-	-
RLH_014	91	52	-
RLH_015	196	-	-

Graph 1- Computing Times for manual segmentation.
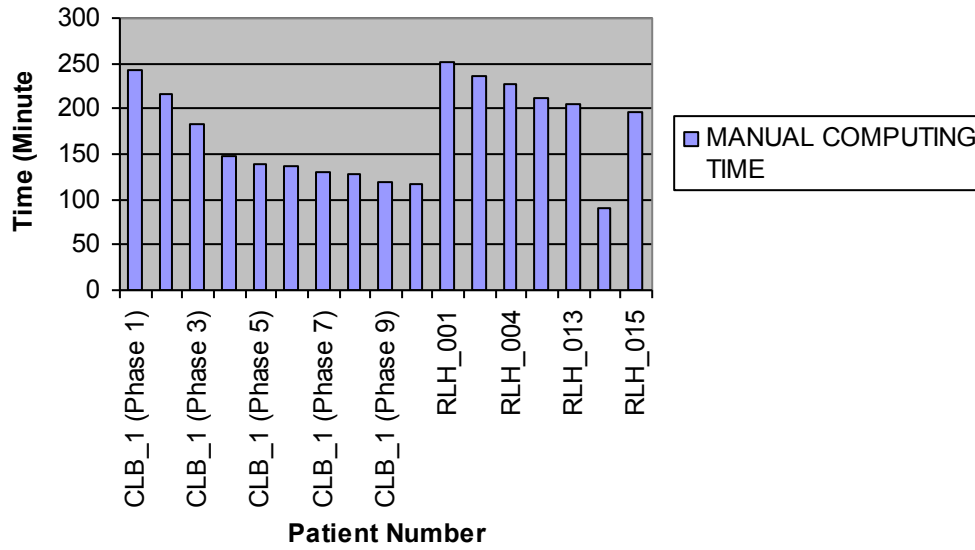
Graph 2- Computing Times for manual segmentation and re-segmentation.
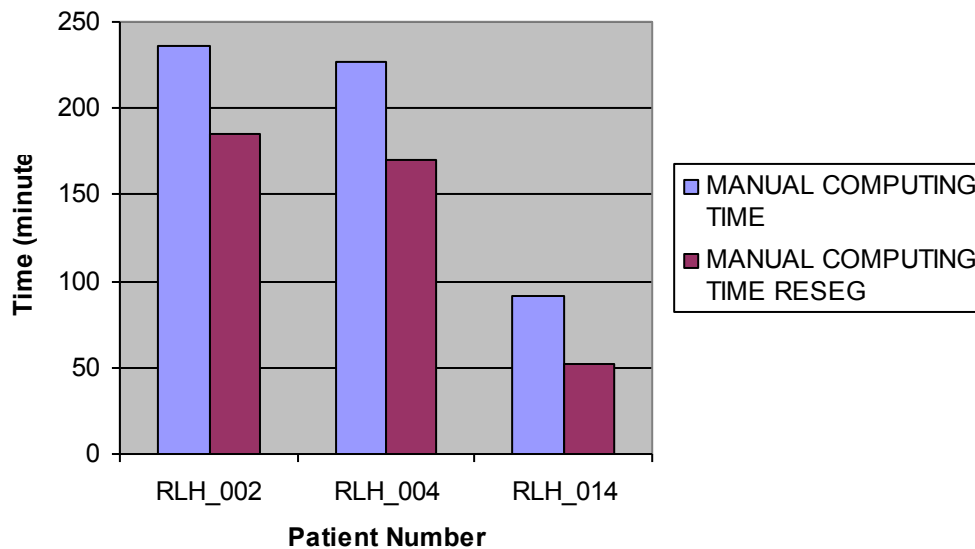
Task Three- Semi-automatic segmentation

Semi-automatic segmentation using ITK-SnAP
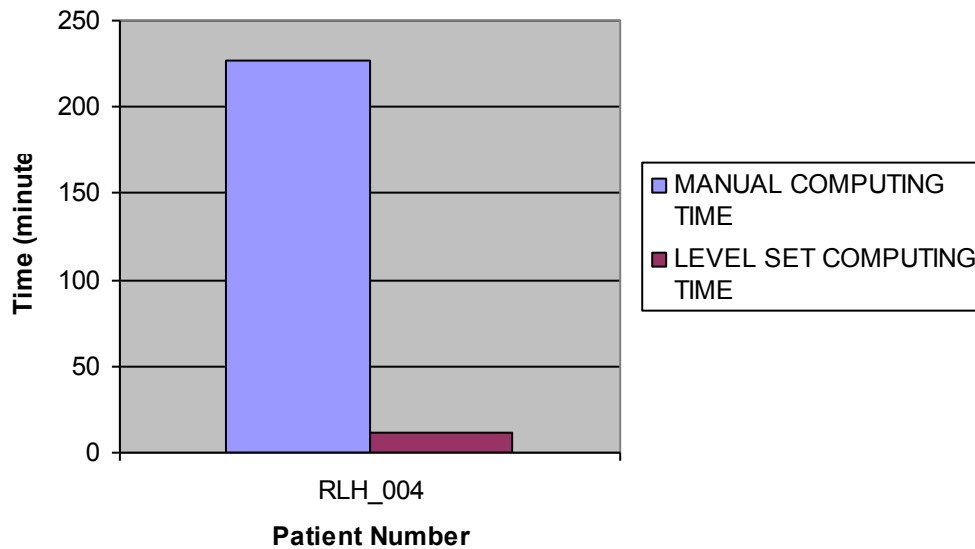
(Image- demonstration of steps involved)
Step 1- Identifying the liver and placing bubbles in the image.
Step 2- Bubble growth. (Image- demonstration of leakage)
Step 3- Construction of 3D mesh.

After identifying the liver and placing bubbles within the liver, the following 3D model was constructed using ITK-SnAP semi-automatic segmentation (Image-model).

Graph 3- Computing Times for manual segmentation and level set segmentation.

Semi-automatic segmentation using Hierarchical Segmentation software

(Image- demonstration of steps involved)

Step 1- Identification of liver boundaries and placement of foreground and background markers within the image.

Step 2- Construction of 3D mesh.

After identifying the liver boundaries and placing green seeds in the foreground (liver) and red seeds in the background, the following 3D model was produced using the hierarchical segmentation software (Image- 3D model)

Patient Number	Manual Computing Time (hr:min:sec)	Hseg Computing Time (hr:min:sec)
RLH_004_top	00:02:00	00:03:00
RLH_004_middle	00:10:00	00:24:00
RLH_014_slices 1-5	00:02:00	00:06:00
RLH_014_slices 6- 10	00:06:00	00:13:00
RLH_014_slices 11-15	00:06:00	00:16:00
RLH_014_slices 16-19	00:07:00	00:44:00

Graph 4- Computing Times for manual segmentation and hierarchical segmentation.

**Segmentation Computing Times: Manual Segmentation Vs
Hierarchical Segmentation**
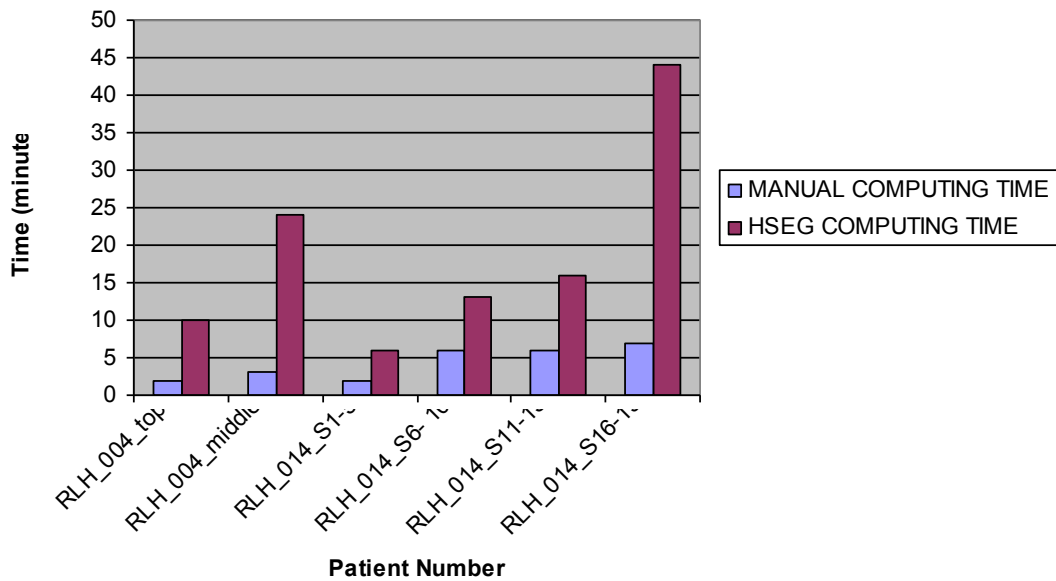
(Edit original graph because the patient numbers are cut off)
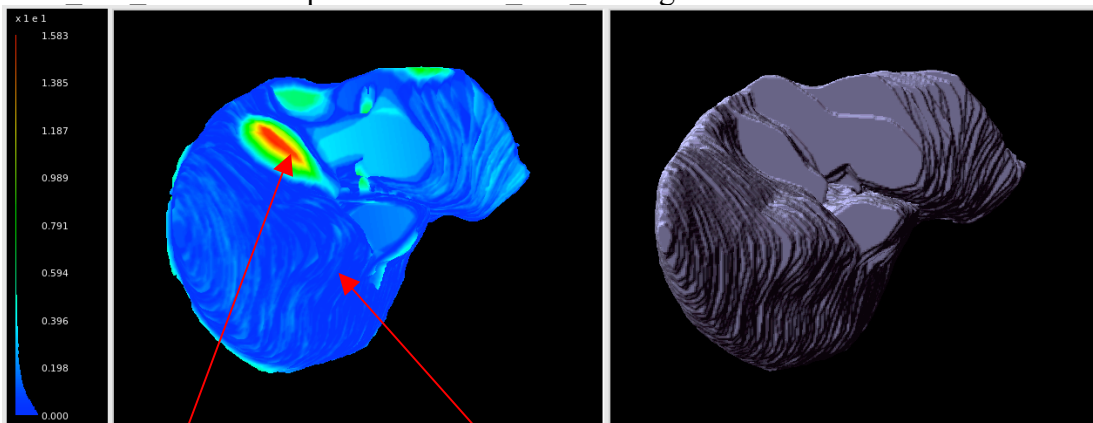
Task Four- Mesh generation

Marching Cubes (Image)

Mesh Alignment (Image of alignment of comparison meshes)

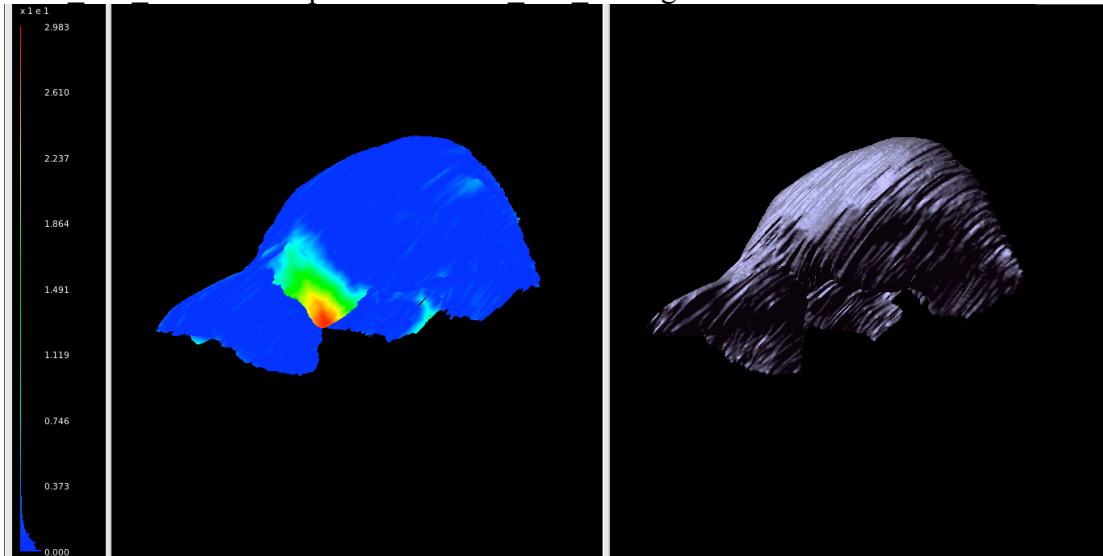## Task Five- Analysis using validation tool M.E.S.H.

M.E.S.H. comparisons:

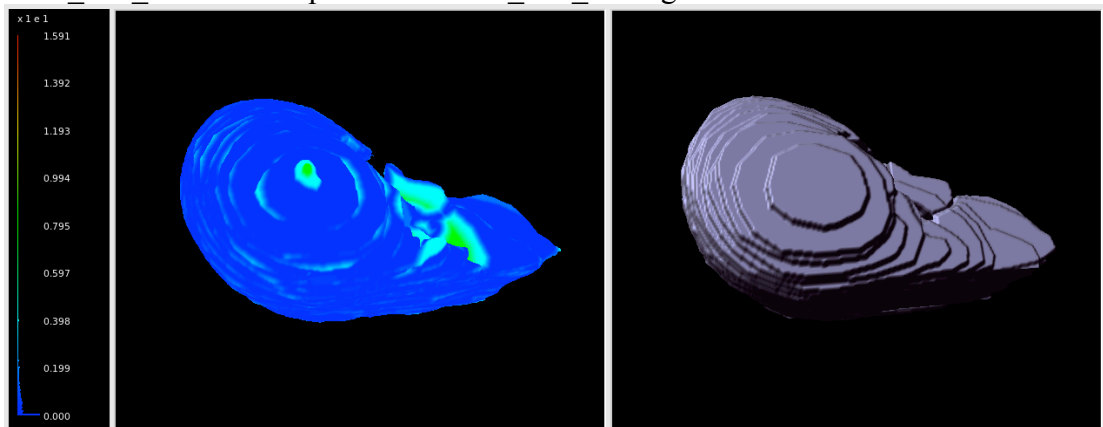RLH_002_Manual comparison to RLH_002_Re-segmentation

The largest difference between   The smallest difference between
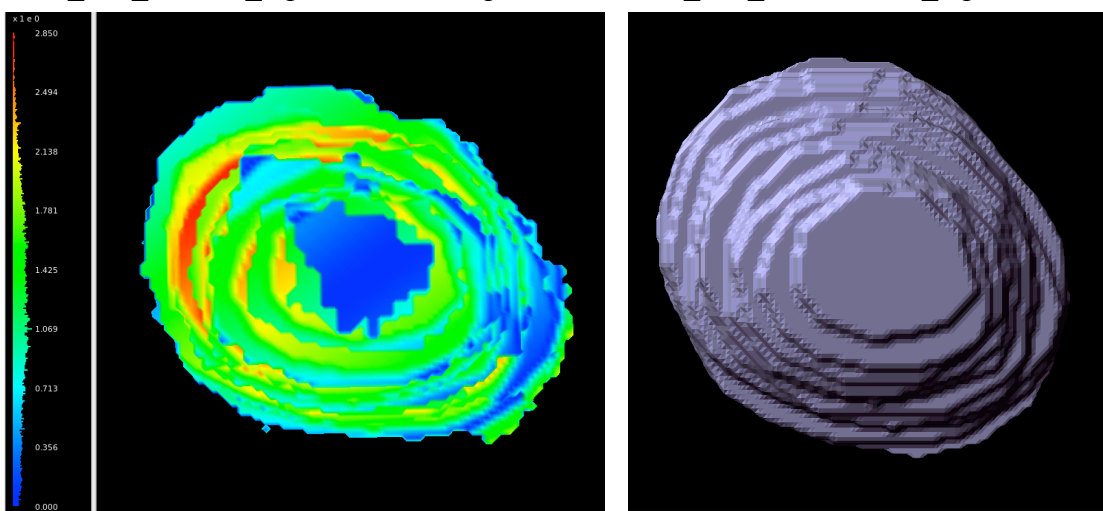the two segmentations   the two segmentations

22

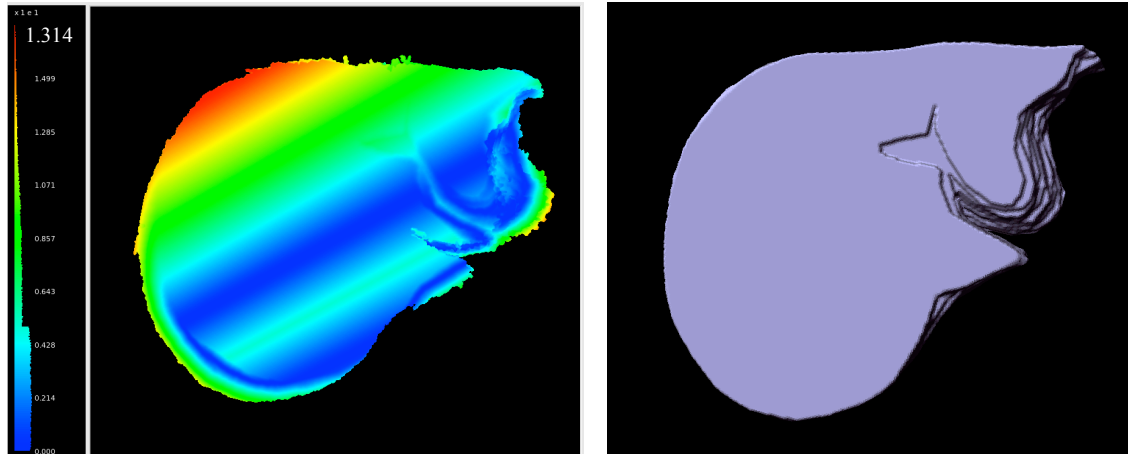RLH_004_Manual comparison to RLH_004_Re-segmentation

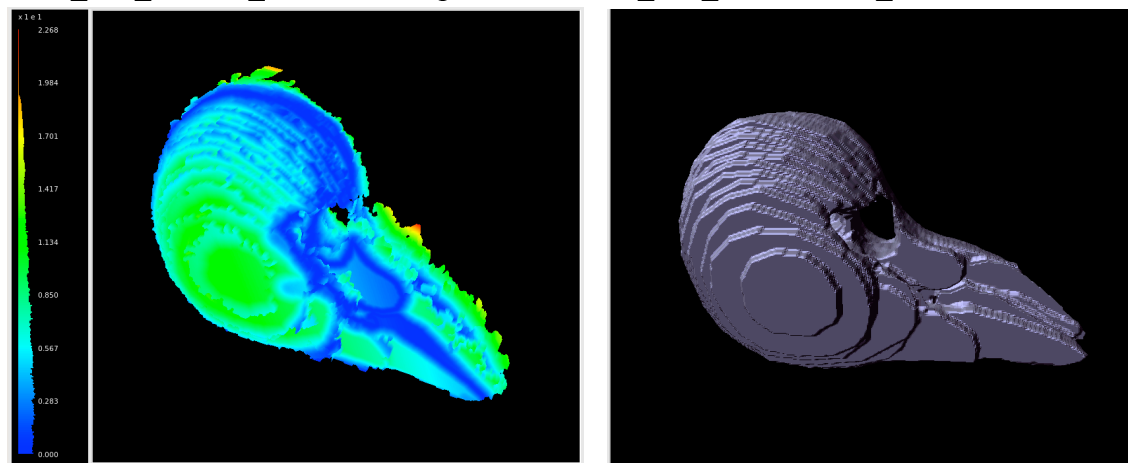RLH_014_Manual comparison to RLH_014_Re-segmentation

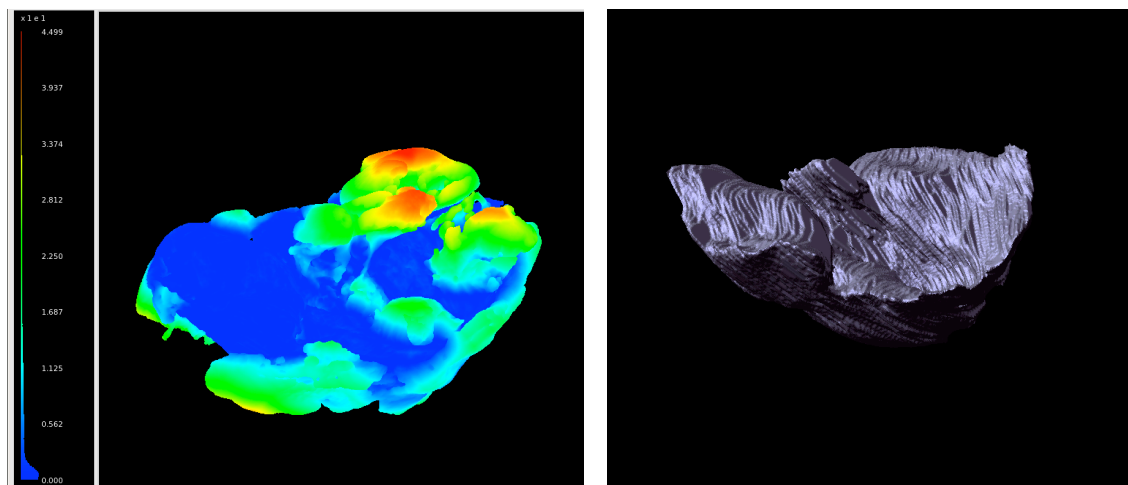RLH_004_Manual_top 10 slices comparison to RLH_004_Hierarchical_top 10 slices

RLH_004_Manual_middle 10 slices comparison to RLH_004_Hierarchical_middle 10 slices

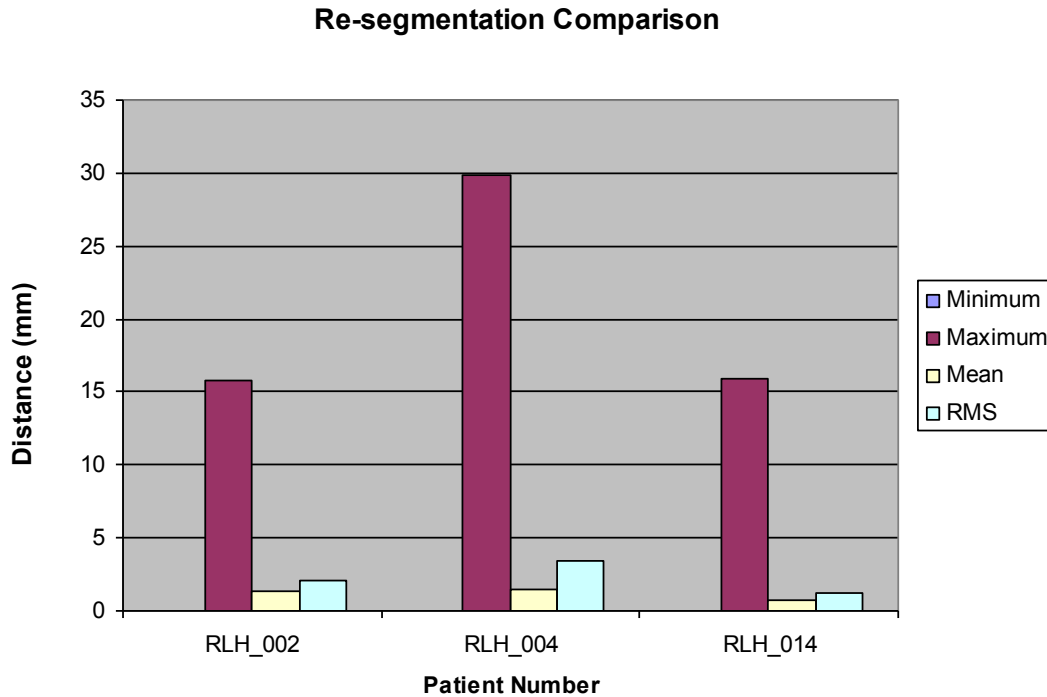RLH_014_Manual_19 slices comparison to RLH_014_Hierarchical_19 slices

RLH_004_Manual comparison to RLH_004_Level set

Patient Number	Distance (minimum)	Distance (maximum)	Distance (mean)	Distance (RMS)
RLH_002	0	15.83	1.32	2.06
RLH_004	0	29.83	1.43	3.45
RLH_014	0	15.91	0.80	1.28

Graph 5- Validation- Comparison between initial manual segmentations and manual re-segmentations.

Re-segmentation Comparison

Patient Number	Distance (minimum)	Distance (maximum)	Distance (mean)	Distance (RMS)
RLH_004_top	0	2.85	1.12	1.26
RLH_004_middle	0	17.14	4.95	6.22
RLH_014_19 slices	0	22.68	6.57	8.08
RLH_004_level set	0	44.99	8.49	12.65

Graph 6-
Validation- Comparison between initial manual segmentations and hierarchical segmentations and initial manual segmentation and level set segmentation.

Resegmentation Comparison
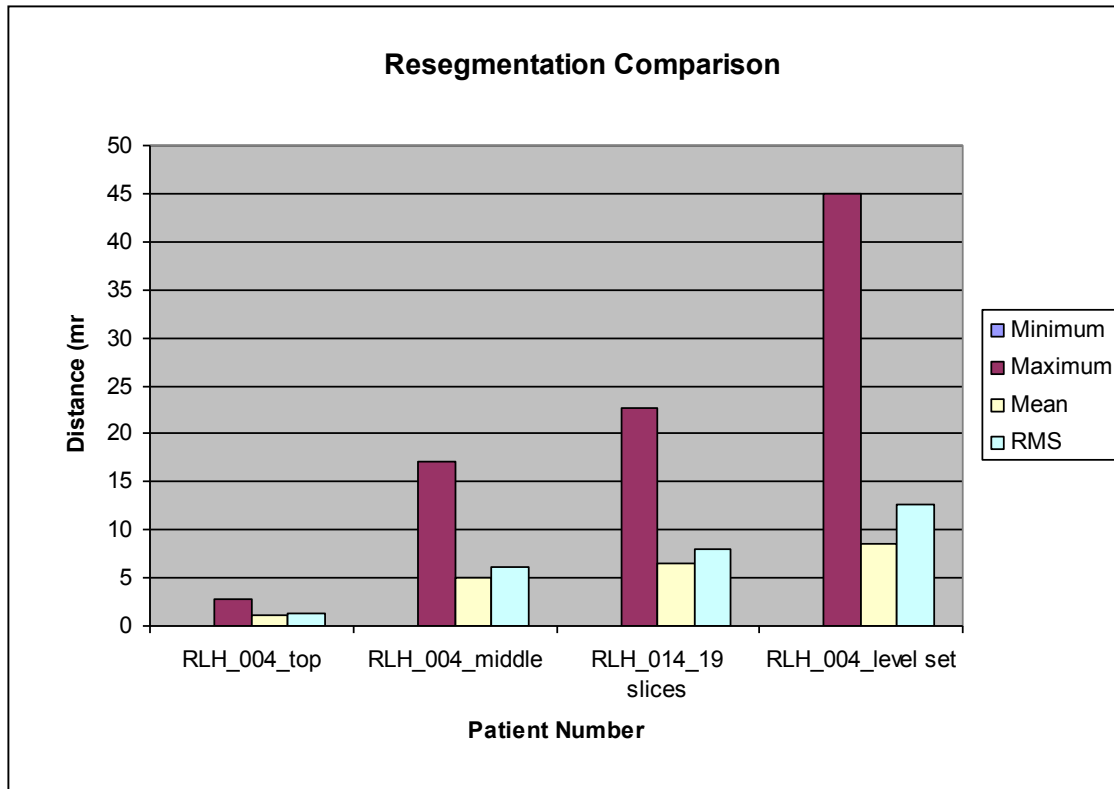
DISCUSSION

Discussion of Results

Task One

Segmentation is a time-consuming process, initially taking between three and four hours to segment a half liver, which consisted of 41 slices on average. The results indicate that as one familiarises themself with the ITK-SnAP software, the process of segmentation and the liver anatomy, the time to segment a liver decreases, with a half liver taking around two hours and a whole liver segmentation (on average 228 slices) taking around between three and four hours. The results also indicate that MR images (data set 014) take less time to segment compared to CT image, despite it taking longer to segment each slice due to ambiguous liver borders. This is due to the smaller quantity of MRI slices, each of which was 4mm thick compared to CT slices being **1-2mm** thick (**Graph 1**).

Re-segmentation was a much faster process than the initial segmentation attempts, due to established familiarity with ITK-SnAP and the liver anatomy (**Graph 2**). The process of segmentation is often error-prone and operator dependent. Discrepancies between segmentations produced by different operators, as well as between repeated attempts by a single operator often occur. Discrepancies often occur due to difficulties in distinguishing the liver boundaries, as the surrounding organs have similar intensity distributions. Re-segmentation of previously segmented data sets allows the operator to make comparisons between their first and second attempt at segmenting exactly the same data set(s) **(MOVE)**.

Despite the level set method on ITK-SnAP being faster than manual segmentation, taking only 12 minutes (**graph 3**), it proved very inaccurate due to leakage of the segmentation label into the surrounding structures and subsequently including them in the mesh (**Figure- leakage**). This was due to ITK-SnAP not being able to differentiate the liver from surrounding structures of similar intensity due to poorly defined liver boundaries, as well as being due to the fact that the initialisation bubbles reach particular liver boundaries before others. Due to the inaccuracy of the subsequent 3D models, we reverted back to using the manual segmentation technique, as it proved more accurate than the semi-automatic method **(Figure/Graph of validation).**

Segmentation of the liver took longer with hierarchical segmentation than with manual segmentation using ITK-SnAP, due to its inability to differentiate between the liver and surrounding structures. A high degree of operator involvement is still required with hierarchical segmentation, with the operator often making several attempts to identify the correct liver boundaries, which the software fails to do, hence increasing the time taken to segment the liver. The results indicate that as the ability to differentiate the liver from the surrounding structures and the complexity of the liver anatomy increase, which is towards the middle of the liver, it takes longer to segment using both hierarchical segmentation and manual segmentation using ITK-SnAP (**Graph 4**).

Limitations of the study

Despite anatomical boundaries of the liver being identified, some structures in close proximity to the liver had similar intensity distributions on the CT and MR images, making the liver boundaries ambiguous. As a consequence these unrelated regions were recognised as being the same region, due to the operator or the hierarchical segmentation software being unable to differentiate between two regions of similar intensity, subsequently creating an unclear edge between the regions. The quality of the image also determines the degree of difficulty associated with successfully segmenting the liver. The MRI (data set 014) was of poor resolution and contrast, making it difficult to identify the liver boundaries. These limitations meant a certain degree of guess-work was required by the operator for manual segmentation.

Nearby organs and tissues have similar intensity distributions to the liver, making the liver's boundaries ambiguous.

Despite being easily understandable and producing high resolution and quality 3D reconstructions of the liver, both ITK-SnAP and the hierarchical segmentation software often crashed in the middle of the segmentation process, meaning data was often lost and consequently needed to be redone. The programme subsequently took time to reopen, thus increasing the workload and slowing down progress. The hierarchical segmentation software was particularly bad, crashing on multiple occasions and despite work being saved, we were unable to reopen it and resume the segmentation process from the slice we had last saved.

Precise segmentation, followed by appropriate visualisation is necessary in the construction of three dimensional models. M.E.S.H. can be used to assess the morphological accuracy of 3D reconstructions of the liver. These 3D models must be able to be modified by incorporating mechanical properties (stiffness, elasticity, mass density, viscoelasticity, friction, stress-strain, cutting force and tensile strength) in order to create a realistic simulator for hepatic surgical procedures.

Segmentation is a time-consuming process, initially taking around 8 hours to segment one liver data set; however, after familiarising oneself with the ITK-SnAP software

and the process of segmentation, a liver segmentation took between 3 to 4 hours to segment.

Improvements in imaging technology will hopefully offer better images for segmentation and construction of 3D models.

Improvements in both ITK-SnAP and the hierarchical segmentation software could include the introduction of a recovery programme, in order to resume segmentations that would otherwise be lost.

DOUBLE SPACE EVERYTHING AND LABEL ALL DIAGRAMS AND REFER TO THEM ALL

References

Aggarwal, R. Moorthy, K. Darzi, A. (2004) Laparoscopic skills training and assessment. *British Journal of Surgery.* Volume 91. Pages 1549-1558.

Aggarwal, R. Grantcharov, T. Moorthy, K. Hance, J. Darzi, A. (2006a) A competency-based virtual reality training curriculum for the acquisition of laparoscopic psychomotor skills. *The American Journal of Surgery.* Volume 191. Pages 128-33.

Aggarwal, R. Grantcharov, T P. Eriksen, J R. Blirup, D. Kristiansen, V B. Funch-Jensen, P. Darzi, A. (2006b) An Evidence-Based Virtual Reality Training Program for Novice Laparoscopic Surgeons. *Annals of Surgery.* Volume 244. Pages 310-314.

Bholat, O S. Haluck, R S. Murray, W B. Gorman, P J. Krummel, T M. (1999) Tactile Feedback is Present During Minimally Invasive Surgery. *Journal of the American College of Surgeons.* Volume 189. Issue 4. Pages 349- 355.

Carter, F J. Schijven, M P. Aggarwal, R. Grantcharov, T. Francis, N K. Hanna, G B. Jakimowicz, J J. (2005) Consensus guidelines for validation of virtual reality surgical simulators. *Surgical Endoscopy.* Volume 19. Pages 1523-1532.

Coleman, J. Nduka, C C. Darzi, A. (1994) Virtual reality and laparoscopic surgery. *British Journal of Surgery.* Volume 81. Pages 1709-1711.

Dawson, S L. & Kaufman, J A. (1998) The imperative for medical simulation. *Proceedings of the **IEEE.*** Volume 8. Pages 479-483.

Delingette, H. (1997) Hepatic Surgery Simulator. *Information Technology in Medicine and Health Care.* ERCIM News. No. 29. **(April)**

Delingette, H. (1998) Toward Realistic Soft-Tissue Modelling in Medical Simulation. *Proceedings of the IEEE.* Volume 86. Issue 3. Pages 512-523.

Delingette, H. Ayache, N. (2005) Creating a simulator for training physicians to perform minimally invasive surgical procedures. Hepatic Surgical Simulation. *Communication of the ACM.* Volume 48. Pages 31-36.

Delp, S L. Loan, J P. Hoy, M G. Zajac, F E. Topp, E L. Rosen, J M. (1990) An interactive Graphics-Based Model of the Lower Extremity to study Orthopaedic Surgical Procedures. *IEEE Transactions on Biomedical Engineering.* Volume 3**7.** Pages 757-767.

Eyler, A E. Dicken, L L. Fitzgerald, J T. Oh, M S. Wolf, F M. Zweifler, A J. (1997) Teaching smoking-cessation counselling to medical students using simulated patients. *American Journal of Preventive Medicine.* Volume 13. Pages 153-8.

Gaba, D M. (2004) The future vision of simulation in health care. *Quality and Safety in Health Care.* Volume 13. Pages 2-10.

Gallagher, A G et al (2001) Ninth annual medicine meets virtual reality conference.

Grantcharov, T P. Kristiansen, V B. Bendix, J. Bardram, L. Rosenberg, J. Funch-Jensen, P. (2004) Randomized clinical trial of virtual reality simulation for laparoscopic skills training. *British Journal of Surgery.* Volume 91. Pages 146-50.

Griffen, L D. Colchester, A C F. Roll, S A. Studholme, C S. (1994) Hierarchical Segmentation Satisfying Constraints. *Proceedings of the British Machine Vision Conference.* Volume 5. Number 1. Pages 135-144.

Haluck, R S. Krummel, T M. Computers and Virtual Reality for Surgical Education in the 21st Century. *Archives of Surgery.* Volume 135. Issue 5. Pages 786-792.

Herman, G T. Liu, H K. (1977) Display of three-dimensional information in computer tomography. *Journal of Computer Assisted Tomography.* Volume 1. Pages 155-160.

www.ifeelpixel.com/pictures/wingmanmouse.jpg

Immersion. www.immersion.com

Koch, A D. Buzink, S N. Heemskerk, J. Botden, S M B I. Veenendaal, R. Jakimowicz, J J. Schoon E J. (2008). Expert and construct validity of the Simbionix GI Mentor II endoscopy simulator for colonoscopy. *Surgical Endoscopy.* Volume 22. Pages158-162.

Kohn, L T. Corrigan, J M. and Donaldson, M S. (2000). *To Err Is Human: Building a safer Health System.* Page 1.

Lityaski, G S. (1999) Profiles in Laparoscopy: Mouset, Dubois and Perissat: the laparoscopic breakthrough in Europe. *Journal of the Society of Laparoendoscopic Surgeons.***Volume**

Liu, A. Kaufmann, C. Ritchie, T. (2001) A computer-based sdimulator for diagnostic peritoneal lavage. *Medicine Meets Virtual Reality.* IOS Press. Pages 279-285.
Lorensen, W E. Cline, H E. (1987) Marching cubes: A high resolution 3D surface construction algorithm. *Computer Graphics.* Volume 21. Issue 4. Pages 163-169.

Marescaux, J. Clement, J M. Tassetti, V. Koehl, C. Cotin, S. Russier, Y. Mutter, D. Delingette, H. Ayache, N. (1998) Virtual Reality Applied to Hepatic Surgery Simulation: The Next Revolution. *Annals of Surgery.* Volume 228. Pages 627-34.

Massie, T. Salisbury, K. (1994) The PHANToM Haptic Interface@ A Device for Probing Virtual Objects. *ASME Winter Annual Meeting.* DSC-Volume 55. Pages 295-300.

McCloy, R. & Stone, R. (2001) Virtual reality in surgery. *British Medical Journal.* Volume 323. Pages 912-915.

Meier, U. Lopez, O. Monserrat, C. Juan, M C. Alcaniz, M. (2005) Real-time deformable models for surgery simulation: a survey. *Computer Methods and Programs in Biomedicine.* Volume 77. Pages 183-197.

Mentice Medical Simulation. www.mentice.com (accesses **April 12 2008).**

M.E.S.H. :http://mesh.berlios.de/

Nesme, M. Faura, F. Payan, Y. (2006) Hierarchial Multi-Resolution Finite Element Model for Soft Body Simulation. *Lecture Notes in Computer Science.* Volume 4072. Pages 40-47.

Paul, Y (2004) ITK-SnAP Integration. *Cognitica Corporation.* **http://www.itksnap.org/docs/viewtutorial.php?chapter=TutorialSectionIntroduction**

Plinkert, P K. Baumann, I. Flemming E. et al. (1998) The use of a vibro-tactile sensor as an artificial sense of touch for tissues of the head and neck. *Minimally Invasive Therapy & Allied Technology.* Volume 7. Pages 111-115.

ProMIS http://www.haptica.com/id44.htm

Salisbury, K. Conti, F. (2004) Haptic Rendering Introductory Concepts**. *IEEE Computer Graphics and Applications.* Pages 24-31.

Satava, R M. (1993) Virtual reality surgical simulator; the first steps. *Surgical Endoscopy.* Volume 7. Pages 203-205.

Schijven, M P. Jakimowicz, J J. (2003) Introducing the Xitact LS500 laparoscopy simulator: toward a revolution in surgical education. *Surgical Technology International.* Volume 11. Pages 32-36.

SensAble http://www.sensable.com/haptic-phantom-omni.htm

SenseGraphics http://www.sensegraphics.com/index.php?page=shop.product_details&flypage=shop.flypage_sensegraphics&product_id=20&category_id=7&manufacturer_id=0&option=com_virtuemart&Itemid=83

Seymour, N E. Gallagher, A G. Roman, S A. ET AL (2002) Virtual reality training improves operating room performance: results of a randomized, double-blinded study. *Annals of Surgery.* Volume 236. Pages 458-464.

Simbionix. www.simbionix.com (accessed **April 12 2008).**

Sorid, D. Moore, S K. (2000) The Virtual Surgeon: Computer-based simulators hone operating skills before the patient is even touched. *IEEE Spectrum.*

Terzopoulos, D. Platt, J C. Barr, H. Fleischer, K. (1987) Elastically Deformable Models. *Proceedings of the Annual ACM. SIGGRAPH '87 Conference. ACM Press.* Volume 21. Pages 205-214.

Vidal, F P. Bello, F. Brodlie, K W. John, N W. Gould, D. Phillips, R. Avis, N J. (2006) Principles and Applications of Computer Graphics in Medicine. *Computer Graphics Forum.* Volume 25. Pages 113-127.

Wilson, M S. Middlebrook, A. Sutton, C. Stone, R. McCloy, R F. (1997) MIST-VR: a virtual reality trainer for laparoscopic surgery assesses performance. *Annals of the Royal College of Surgeons of England.* Volume 79. Pages 403-404.

Wu, X. Downes, M S. Tendick, F. (2001) Adaptive Nonlinear Finite Elements for Deformable Body Simulation Using Dynamic Progressive Meshes. *Eurographics.* Volume 20. Issue 3. Pages 438-448.